Weak localization in superconductors: A study of radiation-damaged Nb₃Ir

K. E. Gray and R. T. Kampwirth

Materials Science and Technology Division, Argonne National Laboratory, Argonne, Illinois 60439

T. F. Rosenbaum and Stuart B. Field

The James Franck Institute and Department of Physics, The University of Chicago, Chicago, Illinois 60637

K. A. Muttalib*

Department of Physics, Brookhaven National Laboratory, Upton, New York 11973

We have studied the critical temperature T_c, upper critical field, and magnetotransport variation as a function of radiation damage in the low-T_c A15 superconductor Nb₃Ir. We find a nonmonotonic variation in T_c with disorder and analyze these results in terms of the competition between density-of-states effects and weak localization. Magnetoresistance measurements confirm the presence of electron interaction effects associated with weak localization.

I. INTRODUCTION

One popular approach for understanding the role of disorder in superconductivity (especially in A15 materials) depends on changes in the density of states (DOS) at the Fermi energy E_F, induced by disorder.[1] Calculations[2] of the DOS of A15 materials show sharp structure near E_F which should smear out with disorder and approach the smoother DOS of the highly disordered amorphous state. This mechanism elegantly explains, and appears to dominate, the experimentally observed increases (decreases) in the transition temperature, T_c of the low-T_c, low-DOS (high-T_c, high-DOS) A15 superconductors as disorder increases.

More recently, the additional role of electron localization in reducing T_c has been discussed.[3-6] Unfortunately, a comparison of these models with experiments on high-T_c materials is difficult because the effects of both DOS changes and localization lead to T_c reductions. Therefore, we have studied a low-T_c A15 superconductor, Nb₃Ir, in which the effects of disorder on T_c through localization and DOS changes are expected to be opposite. A signature of both effects simultaneously occurring would be a nonmonotonic change in T_c with disorder. This is what we found in the results of both α-particle and proton bombardment experiments on Nb₃Ir sputtered films (Fig. 1). Note that the dip in T_c is significantly larger than the resistive transition widths.

Unfortunately the dip by itself does not confirm the nature of the competing effects, only that there are two effects. For example, Schneider et al.[7] propose that their similar results on Nb₃Ir can be explained by invoking a competing effect on T_c of two lattice defects: antisite disorder (which they assume decreases T_c) and small displacements (which they assume increases T_c). Their model requires that the number density of small displacements does not increase linearly with dose for small doses. Instead, we have analyzed our results in terms of a theoretical model of weak localization.[5] Justification for this approach comes from our measurements of magnetoresistance, which show the characteristic dependences on field, H, and normal-state resistivity ρ_N, for the electron interaction effects associated with weak localization.[8]

The weak-localization analysis of superconductivity[5] requires a knowledge of both the electron mean free path, $\hat{l}$, and the electron-phonon coupling constant, λ, which for Nb-based A15 superconductors is proportional to the DOS. The T_c depends most strongly on λ, but measurements of T_c alone cannot determine both parameters. Therefore, we also use measurements of the upper critical field, H_{c2}, near T_c (specifically $H'_{c2} \equiv dH_{c2}/dT$ at T_c), which depend more strongly on $\hat{l}$, to self-consistently determine both parameters for each sample. A final check
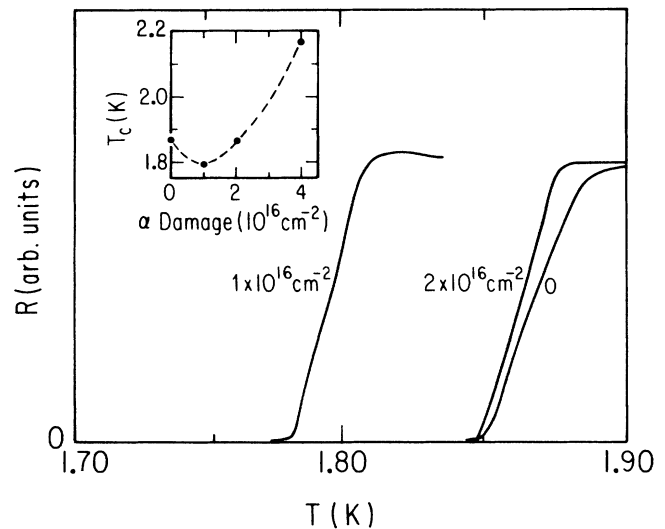

FIG. 1. Resistive transitions of Nb₃Ir films with low dose. Inset: Variation of T_c (defined as midpoint of resistive transition) as a function of α-particle dose.

on the procedure is a comparison of the resistivity calculated from these parameters with the measured ρ_N. The resulting analysis shows λ to be a monotonically increasing function of radiation dose, implying that the dip in T_c is a direct result of a competition between localization and λ changes induced by disorder. Although it is reasonable to assume that λ is proportional to the DOS, we cannot rule out that it is not, and the changes in λ are phononic in origin.

II. SAMPLE PREPARATION
AND CHARACTERIZATION

We have started with well-characterized single-phase samples and use charged-particle (α particles and protons) radiation to decrease the electron mean free path, $\hat{l}$, while maintaining the same overall composition. We therefore avoid potential differences, other than $\hat{l}$, inherent in a series of different "as-made" samples exhibiting different ρ_N. Of the low-T_c $A15$ superconductors, Nb_3Ir has an unusually wide compositional range[9] for the $A15$ phase, reducing the probability of impurity phases.

Films were sputtered from a segmented target using a Varian 5-in.-diameter high-rate magnetron source which has been used[10] previously to produce excellent-quality films of the high-T_c $A15$ superconductors Nb_3Sn and Nb_3Ge (with a segmented target). Wedge-shaped segments of Ir foil, each representing about 3% of the total target, were attached to a Nb target using Nb screws. The sputtering pressure, using Ar, was 27 mtorr to ensure thermalization and mixing of the species (for the 3-in. target-to-substrate spacing used) before condensation onto 1/2-in.-square sapphire substrates (~ 0.022 in. thick), which were centered on the target axis and held at a temperature of ~ 880 °C using a massive heater block. The number of wedges was varied and the resulting films analyzed using x-ray diffraction and Rutherford backscattering, together with measurements of T_c and transition width.

Results of Rutherford backscattering show a linear dependence of the composition ratio (Nb to Ir) varying from 3.5 for 6 wedges to 0.84 for 12 wedges, with a value of 2.85 ± 0.1 for 7 wedges. The lattice constant, determined from x-ray diffraction, varied linearly from 5.153 to 5.095 Å as the number of wedges increased from 6 to 10. The (200) orientation was the strongest of the 8 peaks identified for the $A15$ phase. For 7 wedges the lattice constant of 5.138 Å is somewhat larger than determinations of 5.135 Å for stoichiometric Nb_3Ir in equilibrium, but thin films made by electron-beam codeposition of Nb and Ir also show[11] a slightly expanded lattice. Finally, T_c has been found to vary somewhat irregularly, although monotonically, from ~ 1.6 K for 6 wedges to 3.92 K for 12 wedges. The bulk values quoted[12,13] for Nb_3Ir range from 1.48 K to 1.63 K, including our measurement of 1.56 K on a single crystal available to us. Higher values for resistive transitions in thin films have been reported.[7] For 7 wedges the higher value of about 1.9 K is consistent with the slight deviation from stoichiometry (2.85 instead of 3) and the T_c variation versus composition reported[14] for bulk and thin film Nb_3Ir. These samples also have a

significantly narrower transition width (by a factor of 5–10) than other nearby compositions. The samples made with 10 and 12 wedges exhibited much higher T_c values (3.5–4 K), which were similarly narrow. The origin of this strong enhancement of T_c for the Ir-rich compound is unknown, but because of the vastly different composition it is unlikely to be related to the disorder effect due to radiation damage reported below. On the basis of these results, samples for radiation damage were made using 7 wedges.

Standard photolithography was used to define about 200-μm-wide strips with 6–7 voltage tabs spaced approximately 1 mm apart. Etching was done, with difficulty, using a modified Nb etch at ~ 60 °C. The small samples reduced the variation of initial film properties of the 5–6 sections due to different location under the sputtering target. In addition, the films did not extend over the substrate edges which can cause nonuniformities of radiation damage. The actual damage of the sections was done sequentially using 1.8-Mev α particles or 0.25-Mev protons produced by the Dynamitron facility at Argonne National Laboratory. A thick brass mask was moved along the substrate with the edge always carefully located in the middle of the corresponding voltage tab (~ 60 μm wide). This location was later verified by the change in visual appearance for different damage amounts. One section of each substrate was left undamaged.

Standard x-ray diffraction studies of the damaged films revealed the same 8 peaks found in the undamaged films which could be indexed to the $A15$ structure. There was no evidence of impurity phases, and these peaks were not substantially weaker nor broader even for the most highly damaged sample. Thus it seems unlikely that phase changes (e.g., amorphization) are responsible for the increasing T_c with dose. However, the lattice constant increased with damage by a maximum of about 0.7%.

To determine ρ_N for each individual section, the widths and lengths were measured with a calibrated microscope and the film thicknesses with a Dektak stylus thickness profilometer. The ρ_N values are seen to saturate as a function of dose in the inset of Fig. 2. This saturation could result from several possible causes: (1) achieving the Ioffe-Regel limit[15]—the maximum resistivity occurring for $\hat{l}$ equal to the interatomic spacing, (2) the inability to cause further disorder due to spontaneous recombination of defects,[16] or (3) the competing effects of increasing DOS and decreasing $\hat{l}$ on ρ_N.

To further analyze these possibilities, the following simplification is assumed for these polycrystalline films:

$$\rho_N^{-1} = 2e^2 N(E_F) \langle v_F \rangle \hat{l}/3 \, , \tag{1}$$

where $N(E_F)$ in the DOS of one spin at E_F and $\langle v_F \rangle$ is the Fermi velocity averaged over the Fermi surface. Note that $\langle v_F \rangle$ and $N(E_F)$ are band-structure values, which do not include the electron-phonon coupling renormalization $(1+\lambda)$; however since they have been calculated[2] for Nb_3Ir, an estimate of $\hat{l}$ is possible. Using[2] $\langle v_F \rangle = 3 \times 10^7$ cm s^{-1}, $N(E_F) = 1.6 \times 10^{34}$ spin^{-1} erg^{-1} cm^{-3}, and $\rho_N = 120$ $\mu\Omega$cm, a value of $\hat{l} \sim 10$ Å is found. Returning to the possible causes of saturation, $\hat{l} = 10$ Å is clearly greater than the expected Ioffe-Regel limit, since the
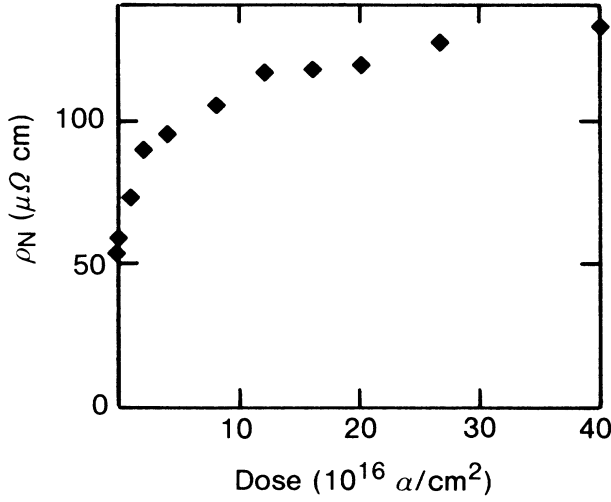
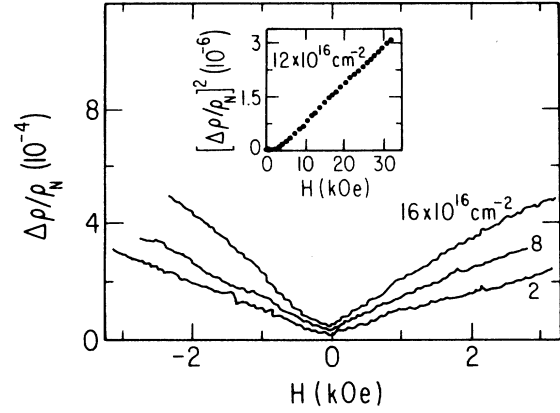FIG. 2. Resistivity of Nb₃Ir films as a function of α-particle dose.

FIG. 3. The magnetoresistance of Nb₃Ir films as a function of magnetic field is shown for various α-particle doses. Inset: Higher field data showing asymptotic $\sqrt{H}$ behavior.

Nb-Nb nearest-neighbor distance is about 2.5 Å which corresponds to $\rho_M \sim 500$ $\mu\Omega$cm.

Spontaneous recombination of defects could limit ρ_N, independent of the Ioffe-Regel limit, and is consistent with the relatively undiminished $A15$ diffraction pattern seen by x rays in the most damaged films. However, the effect of the changing DOS on ρ_N could also contribute since $\hat{l}$ will decrease with damage somewhat faster than ρ_N^{-1} due to the concomittant increase in $N(E_F)$ [see Eq. (1)]. Further discussion of this effect must await the determination of localization parameters and $N(E_F)$ in Sec. V.

III. MAGNETORESISTANCE

The magnetoresistance (MR) was measured with the samples immersed in liquid helium at 4.2 K and in magnetic fields up to 30 kOe which were parallel to the film. The results, shown in Fig. 3 for several samples, indicate a positive MR which asymptotically approaches (inset) the $\sqrt{H}$ dependence expected[8] for weak localization. There are several effects of disorder which can result in a positive MR proportional to $\sqrt{H}$. These include: (i) quantum corrections of the noninteracting electron system[17] for a high spin-orbit scattering rate (which is expected for Nb₃Ir), (ii) the quantum corrections of the interacting system[8] for a net repulsive electron interaction, (iii) spin splitting[18] of the conduction electrons, and (iv) the electron-electron interaction[19] which modifies the effect of superconducting fluctuations[20] on the conductance. In all these cases the MR is small for $H \lesssim H_x$, where H_x is the appropriate crossover field for each effect.

In cases (ii) and (iii) above, our data can be fit to the appropriate functional form, but with a crossover field which is two orders of magnitude smaller than the expected values. These expected crossover fields are

$$H_{x,b} = \pi c k_B T / 2eD ,\tag{2}$$

where D is the actual diffusion constant:

$$D = \langle v_F^* \rangle \hat{l}/3\tag{3}$$

which is derived from the electron-phonon renormalized Fermi velocity, $\langle v_F^* \rangle = \langle v_F \rangle /(1+\lambda)$, and

$$H_{x,c} = k_B T / g\mu_B .$$

Therefore the contributions from (ii) and (iii) are negligible at the field values of our experiments. Because of the large spin-orbit scattering rate expected for Nb₃Ir, both (i) and (iv) will give a positive contribution to MR and have the same functional form:[19]

$$\frac{\delta\rho}{\rho_N} = \frac{[\beta(T)-\alpha]}{\pi^2} \left[\frac{\rho_N e^2}{2\hbar}\right]^{3/2} [N(E_F)(1+\lambda)\hbar/\tau_i]^{1/2}$$

$$\times [h^{1/2} f_3(h)] ,\tag{4}$$

where $h = H/H_{x,a}$, $H_{x,a} = \hbar c/4eD\tau_i$, τ_i is the inelastic scattering time, and[8]

$$f_3(h) = \sum_{n=0}^{\infty} \{2[(n+h+1)^{1/2}-(n-h)^{1/2}]$$

$$-(n+1/2+h)^{-1/2}\} .\tag{5}$$

Here α represents effect (i), and for a large spin-orbit scattering rate,[19] α equals $-\frac{1}{2}$, while $\beta(T)$ represents effect (iv) and is determined in a manner described in Ref. 19, using our measured T_c. Unfortunately $H_{x,a}$ for these cases contains an unknown τ_i, so that when fitting our data to Eq. (4) (see Fig. 4), the determination of the crossover field alone is insufficient to confirm quantitative agreement. However, the fitting procedure also gives a value of τ_i from the prefactor of Eq. (4). These values are compared in Table I to show the extent of the quantitative consistency. The largest difference is $\sim 40\%$, with τ_i ranging from ~ 0.1 to 0.2 nsec and showing no consistent trends with ρ_N. Experimental uncertainties from noise could account for some of this scatter. We feel that this

agreement reasonably confirms the existence of electron interaction effects associated with weak localization in Nb$_3$Ir.

IV. WEAK LOCALIZATION THEORY AND SUPERCONDUCTIVITY

In zero field, the correction to the superconducting transition temperature calculated by Fukuyama, Ebisawa, and Maekawa[5] (FEM) is given by

$$\ln\left[\frac{T_{c0}(0)}{T_c(0)}\right]=K_0 L^2 , \qquad (6)$$

where $L\equiv(2\pi k_F \hat{l})^{-1}$ is the weak-localization expansion parameter of FEM, k_F is the Fermi momentum, $T_c(0)$ is the measured critical temperature in zero field, $T_{c0}(0)$ is the corresponding (fictitious) value if localization were absent, and

$$K_0=(3\sqrt{3}\pi/2)\left\{2\pi/G+(\mu^*/G)^2\left[\left(\frac{1+\mu \ln(E_F\tau)}{\mu}\right)^2 -2\pi\ln(\omega_D\tau)\right]\right\} , \qquad (7)$$

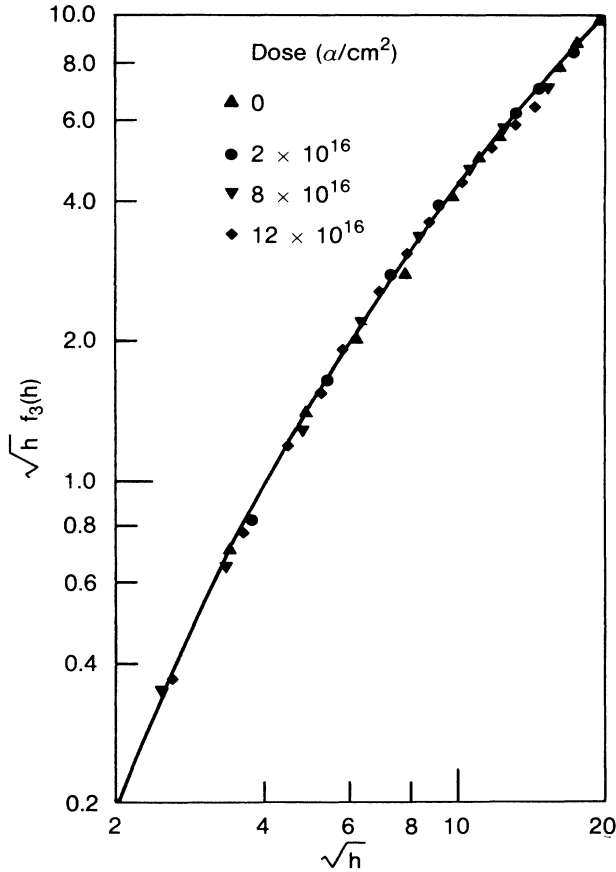where $G\equiv\lambda-\mu^*$ is the net attractive electron-electron in-

FIG. 4. The function $\sqrt{h}f_3(h)$ defined in Eqs. (4) and (5) plotted against $\sqrt{h}$ to emphasize the high-field assymptote. Our data for an undamaged and three damaged films are shown.

TABLE I. Inelastic scattering time obtained by fitting the magnetoresistance data to Eq. (4) for Nb$_3$Ir samples of various resistivities, ρ_N.

ρ_N ($\mu\Omega$ cm)	τ_i (crossover) (nsec)	τ_i (amplitude) (nsec)
60	0.135	0.084
90	0.241	0.157
107	0.136	0.210
118	0.150	0.206

teraction, with μ^* and μ being the screened and unscreened Coulomb parts. Here ω_D is the Debye frequency and $\tau=\hat{l}/\langle v_F^*\rangle$. Because of the relative magnitudes of the terms and the logarithms, K_0 is fairly insensitive to the values used for $E_F\tau$ and $\omega_D\tau$.

We use the McMillan equation, as modified by Allen and Dynes,[21] in place of the BCS equation of FEM for $T_{c0}(0)$:

$$\ln\left[\frac{T_{c0}(0)}{W}\right]=\frac{-1.04(1+\lambda)}{\lambda-\mu^*(1+0.62\lambda)} . \qquad (8)$$

We take[13] $\mu^*=0.13$ since it is only very weakly dependent on the DOS. For Nb$_3$Ir, the value of the characteristic phonon frequency W can be obtained from the work of Junod et al.[13] to be 146.6 K, which we determined[21] for a clean limit value of $\lambda=0.55$.

We cannot proceed further with the above analysis since there are two unknowns λ and L and only one measurement $T_c(0)$. Two other measurements give information about λ and L: the normal state resistivity ρ_N; H_{c2}', the derivative of the upper critical field with respect to temperature in the limit of $T\rightarrow T_c$. From the definition of L and Eq. (1), one finds

$$\rho_N=3.18\times10^{31}\left[\frac{m_{\rm BS}}{m_e}\right]\frac{L}{N(E_F)} , \qquad (9)$$

where $m_{\rm BS}=\hbar k_F/\langle v_F\rangle$ is a band-structure effective mass, m_e the free-electron mass, ρ_N is in units of Ω cm, and $N(E_F)$ does not include the electron-phonon renormalization and is in units of spin^{-1} erg^{-1} cm^{-3}.

The H_{c2}', including localization corrections, can be obtained from the FEM theory[5] by considering the following identity:

$$\ln\left[\frac{T_c(H)}{T_c(0)}\right]\equiv\ln\left[\frac{T_c(H)}{T_{c0}(H)}\right]+\ln\left[\frac{T_{c0}(H)}{T_{c0}(0)}\right]$$

$$+\ln\left[\frac{T_{c0}(0)}{T_c(0)}\right] , \qquad (10)$$

where $T_c(0)$ and $T_c(H)$ are the measured critical temperature in zero field and applied field H, including the effects of localization, and $T_{c0}(0)$ and $T_{c0}(H)$ are the corresponding (fictitious) values if localization and interaction effects were absent. The second term on the right-hand side is the result of the usual Ginzburg-Landau-Abrikosov-Gor'kov (GLAG) theory[22] and the other two terms

represent corrections due to weak localization calculated by FEM in zero field and in applied field H. In the combined limits of dirty superconductivity, low field $(H \rightarrow 0)$ and weak localization $(L \rightarrow 0)$, one finds

$$H_{c2}' = \frac{H_{c2}'(\text{GLAG})}{1 - \sqrt{3}\pi^2 L^2} , \qquad (11)$$

where H_{c2}' (GLAG) is the result of GLAG theory in the dirty limit [see Eq. (13) below]. Note that the result of FEM (Ref. 5) contains a typographic error, omitting the last two terms of their crucial Eq. (2.14). The correct equation[23], which we use, is, in the terminology of FEM, given by

$$\ln \left[\frac{T_c(H)}{T_{c0}(H)} \right] = \frac{\delta K(T_c(H))}{N(E_F)} + \psi \left[\frac{1}{2} + \frac{a}{4\pi T_{c0}(H)} \right]$$
$$- \psi \left[\frac{1}{2} + \frac{a}{4\pi T_c(H)} \right] ,$$

where $\delta K(T)$ is Eq. (2.15) of FEM, ψ is the digamma function and $a = 2DeH/c$. Note also that for $L = 0$, one recovers the usual GLAG result and the effect of localization is to increase H_{c2}' above the GLAG value.

Note also that for small L, Eq. (6) reduces to

$$T_c(0) = T_{c0}(0)(1 - K_0 L^2) , \qquad (12)$$

from which the effects of weak localization on H_{c2}' and T_c can be directly compared. In Eq. (7), one finds that K_0 is dominated by the first term in curly brackets which is $3\sqrt{3}\pi^2/G$ and hence $3/G$ times the coefficient of L^2 in Eq. (11) for H_{c2}'. For Nb$_3$Ir, $G \sim 0.5$ so the effect on H_{c2}' is about 6 times smaller than that on T_c. However, for Nb$_3$Sn, with[24] $G \sim 1.8$, the effects are more nearly equal.

The standard expression from GLAG theory gives[24]

$$H_{c2}'(\text{GLAG}) = -\frac{12\pi}{7\zeta(3)} \frac{k_B c}{1.17e} \frac{1}{\langle v_F^* \rangle \hat{l}}$$

$$= -3.83 \times 10^4 \rho_N \gamma \qquad (13)$$

assuming no strong-coupling correction, and γ is the coefficient of the linear term of the specific heat in ergs/cm^3/K^2. From the definition of L and Eq. (1), one finds

$$H_{c2}'(\text{GLAG}) = -179 \left[\frac{m_{\text{BS}}}{m_e} \right] (1+\lambda) L , \qquad (14)$$

in units of kOe/K. Comparing this to Eq. (9), the use of H_{c2}' to determine L seems beneficial because $N(E_F)$ is not needed. In addition, ρ_N may be influenced by defects which are not intrinsic to the damaged Nb$_3$Ir itself. For example, surface cracks at high doses can result from substrate expansion due to the buildup of He gas. The surface of the highest dose samples had a somewhat crazed appearance.

In order to use Eq. (14) to obtain L, the clean-limit value, $H_{c2}'(0)$, must be subtracted from the measured H_{c2}' and the FEM localization correction [see Eq. (11)] applied. From Ref. 24, we find

$$H_{c2}'(0) = -2.71 \times 10^{13} T_c / \langle v_F^* \rangle^2 , \qquad (15)$$

where $\langle v_F^* \rangle = \langle v_F \rangle /(1+\lambda)$ includes the electron-phonon renormalization, and the strong-coupling correction is ignored. For the clean Nb$_3$Ir single crystal, $T_c \cong 1.5$ K and the band-structure calculations[2] give $\langle v_F \rangle$ and λ so that $\langle v_F^* \rangle \simeq 2 \times 10^7$ cm s^{-1} and $H_{c2}'(0) \cong 100$ Oe/K. Similar small values are calculated for the damaged and undamaged films. These corrections are small for Nb$_3$Ir and are summarized by

$$H_{c2}' - H_{c2}'(0) = -179 \left[\frac{m_{\text{BS}}}{m_e} \right] (1+\lambda) L /(1 - \sqrt{3}\pi^2 L^2) .$$
$$(16)$$

The procedure starts by choosing a value of m_{BS}, which is presumed the same for all samples (doses). Next, an iteration is performed to determine λ and L. First a λ value is guessed and L is found from Eq. (16). Next $T_c(0)$ is computed from Eqs. (6)–(8) and compared with the measured value. Then λ is modified accordingly, and the procedure repeated until convergence. This is done for each sample, and checked by the constancy of the ratio of the measured resistivities to those calculated from Eq. (9) [using for the first and only time in the analysis, the fact that $N(E_F)$ is proportional to λ]. On this basis, m_{BS} is adjusted for the smallest deviation of the ratio, and the magnitude of $N(E_F)$ can be determined as that value which brings the ratio to one [see Eq. (9)].

V. MEASUREMENTS AND ANALYSIS

Resistive transitions were determined using standard four-terminal low-frequency ac techniques with the samples immersed in liquid helium. The sample temperature was slowly drifted through the transition and was determined from vapor pressure measurements at the top of the 10-cm-diameter Dewar. Values were reproducible from run to run, indicating no effects of thermal cycling nor chemical attack on these very robust, tenacious films. Resistive transitions were sharp (see Fig. 1) even at high fields and the criterion of half the normal-state resistance was used to evaluate T_c. The zero-field data for all samples is presented in Fig. 5. The low value for the bulk single crystal is, no doubt, due to the films being slightly off stoichiometry (see Sec. II). Finite fields were applied perpendicular to the film plane in order to avoid surface superconductivity (significantly higher critical fields were found for parallel fields) and were provided by a small superconducting solenoid. To obtain H_{c2}', measurements up to 10 kOe were sufficient as there is *no* difference between the zero-field $T_c(0)$ and the extrapolation of $T_c(H)$ to within the random scatter of measurements ($\sim$3-4 mK). This unusual behavior indicates that each sample is reasonably uniform and free of large-scale inhomogeneities. Values of H_{c2}' for all the samples are plotted in Fig. 6 together with the first measurement of a bulk single crystal. For this single crystal the zero-field $T_c(0)$ of 1.56 K was significantly larger than the H_{c2} extrapolation which was 1.53 K. While ρ_N for this somewhat irregularly shaped crystal was difficult to determine accurately, the

data point reinforces the linear extrapolation of H'_{c2} to a very low value in the clean limit ($\rho_N \rightarrow 0$). Recall that $H'_{c2}(0) \sim 100$ Oe/K results from Eq. (15) using the previously mentioned band-structure calculations[2] of $\langle v_F \rangle$ and λ together with $T_c = 1.5$ K. Our measurement in the single crystal clears up the discrepancy noted in Ref. 2 by providing, for the first time, critical field data in the clean limit for Nb$_3$Ir. Confirmation of the very low $H'_{c2}(0)$ also validates the use of the dirty limit of GLAG in the FEM theory.

The analysis proceeds as outlined in the preceding section. The fit is not very sensitive to (m_{BS}/m_e), so we set it equal to one for the results presented below. The ratio of the calculated to measured resistivity is closest to one if the DOS in the clean limit is about 1.35×10^{34} spin^{-1}erg^{-1}cm^{-3}, i.e., about 15% lower than the calculated value.[2]

The results for λ are plotted against L in Fig. 7 together with the values of λ obtained from Eq. (8) in which localization effects are absent. Figure 7 shows that when localization effects are included, λ is a monotonically increasing function of L (and hence radiation dose). Therefore, we conclude that the dip in T_c can be explained as a direct result of the competition between localization and λ (or DOS) changes induced by disorder.

Returning to the question of resistivity, we can now say more. According to the Ioffe-Regel criterion[15] we expect saturation when $\hat{l} = a_0/2$ where $a_0 = 5.140$ Å is the unit-cell dimension, which is twice the Nb-Nb separation. The maximum value of L in this case is given by

$$L_M = (\pi k_F a_0)^{-1} .$$

Using $m_{BS} = m_e$ and the calculated[2] $\langle v_F \rangle$, one finds $L_M = 0.238$. The localization fit for our most damaged films indicate $L \cong 0.053$, implying $\hat{l} \cong 11.5$ Å which corresponds to $\rho_N \cong 105$ $\mu\Omega$ cm from Eq. (1). Although we measured values up to 130 $\mu\Omega$ cm, these values may be artifically high due to substrate crazing caused by gas buildup during irradiation at such high doses [(1-4)$\times 10^{17}$ α cm^{-2}].

Thus, we reinforce our conclusion that the saturation of the ρ_N with dose shown in Fig. 2 is not due to the Ioffe-Regel limit, but rather a saturation of our ability to do further damage with particles due to spontaneous recombination of defects. The behavior of T_c with dose (see Fig. 5) is therefore curious, since the largest changes in T_c occur as ρ_N is beginning to saturate. Including the DOS effect on ρ_N, which is given by Eq. (1) [or Eq. (9)], has little effect, although the changes of $N(E_F) \rho_N$ with dose are greater than ρ_N alone due to the increasing $N(E_F)$ with dose. Apparently the sensitivity of λ to disorder increases significantly for very disordered Nb$_3$Ir.

VI. LOCALIZATION ANALYSIS OF Nb$_3$Sn

This same analysis can be applied to the published measurements[24-26] on another A15 superconductor, Nb$_3$Sn.
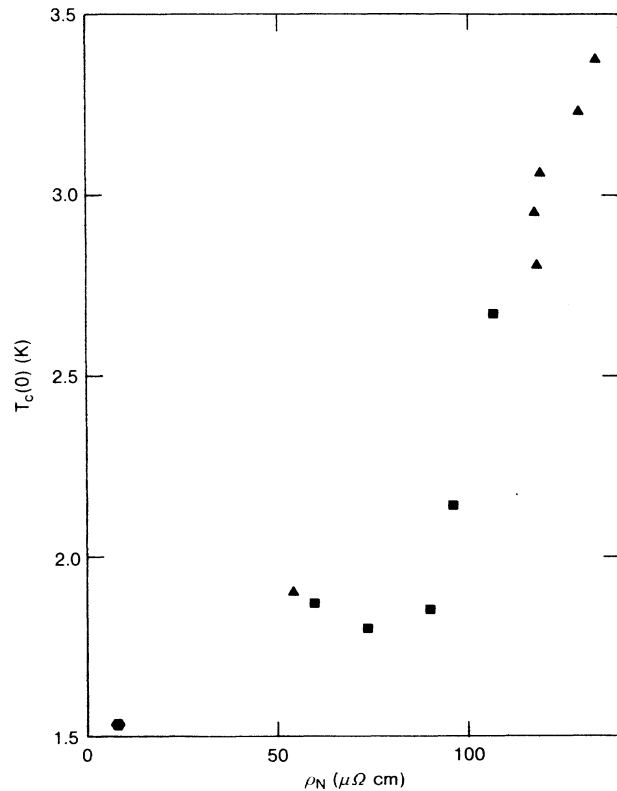

FIG. 5. The superconducting transition temperature in zero applied magnetic field as a function of measured resistivity. In this figure and Figs. 6 and 7, the squares (triangles) represent different sections of one (another) sample which were irradiated to different doses, with the lowest resistivity data representing undamaged sections. The hexagon is a bulk single crystal.
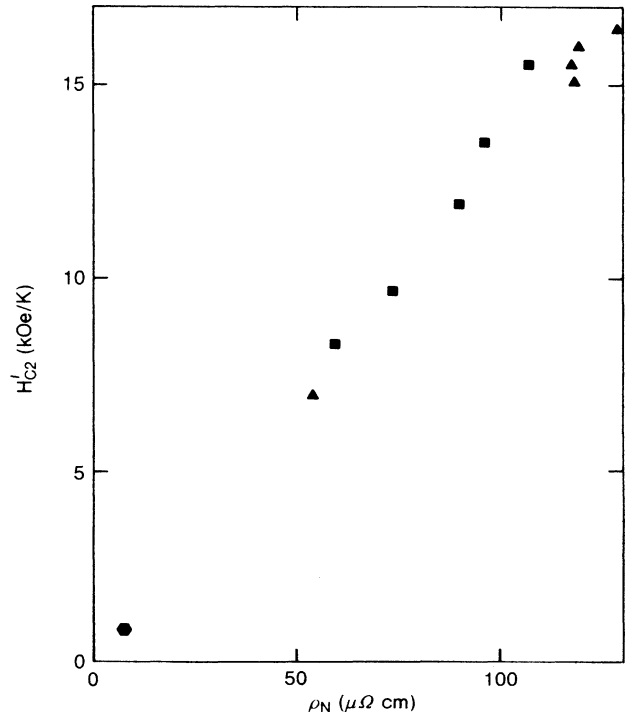

FIG. 6. The measured critical field slope H'_{c2} plotted against measured ρ_N. Symbols the same as in Fig. 5.

This is a high-T_c material in which the DOS is expected to decrease with disorder. Another difference from Nb$_3$Ir is the significantly higher $H'_{c2}(0)$ due to the high T_c (~ 18 K) and large value of λ (~ 1.8). This is seen in Eq. (15) and the experimental values of H'_{c2}, which extrapolate to about 14 kOe/K, i.e., about 140 times larger than Nb$_3$Ir. As a result the variation of $H'_{c2}(0)$ with disorder, for use in Eq. (16), is significant. The above localization analysis does not determine the variation of $\langle v_F \rangle$ with disorder so a reasonable assumption is needed. We choose $\langle v_F \rangle^{-1}$ proportional to $N(E_F)$, and hence λ, since $N(E_F)$ is the Fermi surface average of $1/v_k$, but remind the reader that this assumption is far from rigorous. Again, obtaining an acceptable fit does not place strong constraints on the parameters. Thus $\langle v_F \rangle = 1.5 - 1.8 \times 10^7$ cm s^{-1} and $m_{BS}/m_e \gtrsim 1$ all yield $N(E_F)$ within 5–10 % of the calculated[13] and measured[13] values of about 3.1×10^{34} spin^{-1} erg^{-1} cm^{-3}.

VII. SUMMARY AND CONCLUSIONS

We have analyzed the transport properties and superconductivity as a function of disorder in Nb$_3$Ir films. Disorder was increased by charged particle irradiation to avoid random compositional changes in as-made films. The wide compositional range[9] for the A15 structure in Nb$_3$Ir greatly reduced the possibility of second crystallographic phases. Therefore we expect that the decreasing
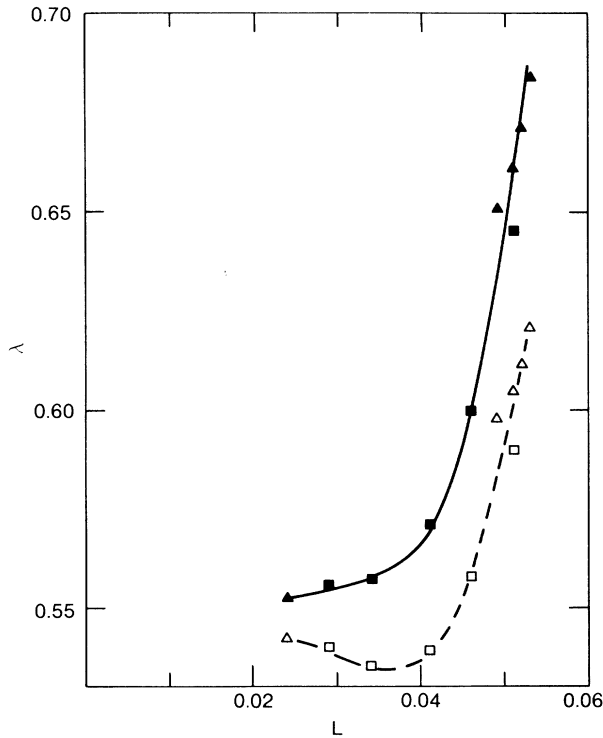

FIG. 7. The calculated electron-phonon coupling constant λ. Open symbols: From T_c measurements using Eq. (8) without localization effects. Solid symbols: From T_c and H'_{c2} measurements using the localization analysis described in Sec. IV.

electron mean free path is the predominant effect of disorder.

The resistivity is found to saturate with particle dose and we conclude that this effect is due to a saturation of our ability to cause further damage because of spontaneous recombination of defects.[16] This is consistent with the relatively undiminished A15 x-ray diffraction pattern in our most damaged films.

The magnetoresistance shows the characteristic field dependence of weak localization[8] and relatively good quantitative agreement is found by including quantum corrections to the noninteracting electron system[17] as well as the effect of electron-electron interactions[19] on superconducting fluctuations. These results give justification to our analysis of superconductivity using the quantum corrections of weak localization theory.[5]

This perturbative theory[5] of weak localization and superconductivity requires two parameters: the electron-phonon coupling, λ; and the weak localization expansion parameter, $L = (2\pi k_F l)^{-1}$. Thus, measurements of two independent properties which depend on L and λ are required. We use the transition temperature, T_c and critical field slope, H'_{c2}. As a function on increasing disorder, T_c drops slightly before increasing dramatically, while H'_{c2} increases monotonically and extrapolates back to the very small value predicted for the clean limit by band-structure calculations.[2] Our additional measurements on a clean, single crystal of Nb$_3$Ir confirm this small value of H'_{c2} and clear up past uncertainty[2] about that point.

A third relevant property, the resistivity, is used to show that the iterated weak localization solutions are consistent as a function of disorder. They also yield a value for the density of states close to band structure calculations[2] and determinations from specific-heat measurements.[2]

It is found that the values of λ thus determined increase monotonically with disorder, so that the dip in T_c can be explained as a direct result of the competition between weak localization and λ (or DOS) changes induced by disorder.

*Present address: Department of Applied Physics, Yale University, New Haven, CT 06520.

[1] L. R. Testardi and L. F. Matthiess, Phys. Rev. Lett. 41, 1612 (1978).

[2] T. Jarlborg, A. Junod, and M. Peter, Phys. Rev. B 27, 1558 (1983).

[3] P. W. Anderson, K. A. Muttalib, and T. V. Ramakrishnan, Phys. Rev. B 28, 117 (1983).

[4] L. Coffey, K. A. Muttalib, and K. Levin, Phys. Rev. Lett. 52, 783 (1984).

[5] H. Fukuyama, H. Ebisawa, and S. Maekawa, J. Phys. Soc. Jpn. 53, 3560 (1984).

[6] A. Kapitulnik and G. Kotliar, Phys. Rev. Lett. 54, 473 (1985).

[7] R. Schneider, G. Linker, O. Meyer, M. Kraatz, and F. Wüchner, in LT-17, edited by U. Eckern, A. Schmid, W. Weber, and H. Wuhl (Elsevier, Amsterdam, 1984), p. 611.

[8] B. L. Al'tshuler, A. G. Aronov, A. I. Larkin, and D. E. Khmel'nitskii, Zh. Eksp. Teor. Fiz. 81, 768 (1981) [Sov. Phys.—JETP 54, 411 (1981)].

[9] F. A. Shunk, Constitution of Binary Alloys, Second Supplement (McGraw-Hill, New York, 1969), p. 188.

[10] R. T. Kampwirth, C. T. Wu, and J. W. Hafstrom, Adv. Cryogenic Eng. 24, 315 (1977).

[11] A. H. Dayem, T. H. Geballe, R. B. Zubeck, A. B. Hallak, and G. W. Hull, Jr., J. Phys. Chem. Solids 39, 529 (1978).

[12] P. Spitzli, Phys. Kondens. Mater. 13, 22 (1971).

[13] A. Junod, T. Jarlborg, and J. Muller, Phys. Rev. B 27, 1568 (1983).

[14] R. Flükiger, H. Küpfer, J. L. Jorda and J. Muller (unpublished).

[15] A. F. Ioffe and A. R. Regel, Prog. Semicond. 4, 237 (1960).

[16] H. Wenzl, in Vacancies and Interstitials in Metals, edited by A. Seeger, D. Schumacher, W. Schilling, and J. Diehl (North-Holland, Amsterdam, 1970), p. 391.

[17] A. Kawabata, Solid State Commun. 34, 431 (1980).

[18] P. A. Lee and T. V. Ramakrishnan, Phys. Rev. B 26, 4009 (1982).

[19] A. I. Larkin, Pis'ma Zh. Eksp. Teor Fiz. 31, 239 (1980) [JETP Lett. 31, 219 (1980)].

[20] K. Maki, Prog. Theor. Phys. Jpn. 39, 897 (1968); 40, 193 (1968); R. Thompson, Phys. Rev. B 1, 327 (1970).

[21] P. B. Allen and R. C. Dynes, Phys. Rev. B 12, 905 (1975).

[22] See, e.g., N. R. Werthamer, in Superconductivity, edited by R. D. Parks (Marcel Dekker, New York, 1969), Vol. 1, p. 321.

[23] H. Fukuyama (private communication).

[24] T. P. Orlando, E. J. McNiff, Jr., S. Foner, and M. R. Beasley, Phys. Rev. B 19, 4545 (1979).

[25] A. K. Ghosh and M. Strongin, in Superconductivity in d- and f-Band Metals, edited by H. Suhl and M. B. Maple (Academic, New York, 1980), p. 305.

[26] C. Nölscher and G. Saemann-Ischenko, Phys. Rev. B 32, 1519 (1985).